

Irradiation-induced densification of cluster-assembled thin films

K. Meinander* and K. Nordlund

Department of Physics, University of Helsinki, P.O. Box 43, FI-00014 Helsinki, Finland

(Received 30 September 2008; published 14 January 2009)

The growth and modification of nanocluster-assembled thin films were studied using molecular-dynamics simulations. Porous thin films of copper were grown through sequential deposition of 50 Cu₇₁₁ nanoclusters on a Cu (100) substrate. Irradiation of these films with Xe and Au ions, at energies ranging 5–30 keV, was then carried out with the aim of increasing their density. Results show that heavy-ion irradiation can successfully be used in the densification of initially underdense thin films. With ion ranges tuned to the thickness of the thin films, densities approaching that of bulk copper were achieved at fluences as low as 50×10^{12} ions/cm². Densification was caused by local melting in individual clusters and the resulting viscous flow of atoms into voids within the films. Nanocrystallinity was preserved as recrystallization occurred according to crystal orientations of the pre-existing clusters.

DOI: 10.1103/PhysRevB.79.045411

PACS number(s): 79.20.Rf, 61.46.Bc, 61.82.Rx, 68.55.-a

I. INTRODUCTION

Nanoclusters have recently been suggested for use in the growth of nanostructured thin films.^{1–3} Due to their inherent nanocrystalline structure, deposition with size-selected nanoclusters should result in the growth of thin films with grains in the same size range as the clusters. Thin-film growth by cluster deposition is also a very gentle technique, suitable for virtually any substrate, as deposition can occur at room temperature or lower, with very low deposition energies.

Thin films grown by low-energy cluster deposition are, however, in general extremely porous, and therefore exhibit very poor adhesion and mechanical properties.² An increase in deposition energy will result in the growth of denser films with better qualities. This may, however, sometimes be harmful toward the substrate, and will almost inevitably destroy any likelihood of the formation of grain boundaries within the films.^{4–6} In some rare cases, if cluster sizes are small enough, epitaxial alignment of clusters can occur even at low deposition energies.^{7–9} Deposition in this manner may lead to the growth of dense thin films, although these films will undoubtedly lack any nanostructure whatsoever.

One option for increasing the density of cluster-assembled thin films is high-temperature annealing.¹⁰ Global melting of the cluster films is however a very destructive technique if nanocrystallinity is to be preserved. At higher temperatures, clusters will sinter, causing a rapid increase in grain size. Thermal annealing can also be harmful for many substrates, as samples are held at elevated temperatures for a considerable duration of time. High pressure compaction is an alternative method, which possesses almost all of the same disadvantages.¹¹

A more gentle method may be irradiation with heavy ions. The effects of heavy-ion irradiation in matter have been a topic of vigorous research during the past century. The deliberate modification of materials through bombardment with ions, be it for the purpose of impurity implantation, defect creation, or structural rearrangement, has become so commonplace that a huge fraction of our modern-day industry relies heavily upon it.¹²

Amorphization and viscous flow, induced by irradiation, in crystalline semiconductors and ceramics have lately been

studied in detail, for purposes as exotic as the activation of human bone replacement materials.^{13–15} Although similar irradiation of close-packed structures, such as face-centered-cubic (fcc) or hexagonal close-packed (hcp) metallic crystals, commonly does more harm than good,¹² through the creation of numerous defects^{16,17} and therein brittleness, we propose its use in the densification of cluster-assembled thin films and hence in the improvement of mechanical properties.

If initially underdense structures are irradiated with heavy ions, local melting and a viscous flow of atoms can result in the filling of voids and hence, a densification of the structure. If recrystallization of molten regions occurs according to local structure of individual clusters, nanocrystallinity can be preserved within the films.

The aim of this work has been to study the feasibility of such a densification of cluster-assembled thin films by heavy-ion irradiation. Molecular-dynamics (MD) simulations were used to evaluate film growth by cluster deposition and the subsequent modification of the porous films by irradiation.

II. METHOD AND SIMULATIONS

Classical molecular-dynamics simulations¹⁸ were used to model the growth of thin films by cluster deposition, and using those films, the interaction between heavy-ion irradiation and porous cluster-assembled structures. Cluster-assembled films were grown through sequential deposition of 50 Cu₇₁₁ clusters on an initially smooth Cu (100) surface. Irradiation of the films was then carried out using Xe and Au projectiles at energies ranging 5–30 keV.

The embedded-atom method (EAM) potential¹⁹ by Foiles *et al.*²⁰ was used to describe the interactions between copper atoms during growth of the cluster films and their irradiation, while EAM cross potentials were used to model the interactions between copper atoms and the gold ions during irradiation. At short distances, the potentials were smoothly joined with the universal repulsive Ziegler-Biersack-Littmark (ZBL) potential.²¹ The ZBL potential was also used to model Cu-Xe interactions during irradiation. Inelastic energy losses due to electronic stopping were included in the calculations

for all atoms with kinetic energy higher than 5 eV.²¹

All simulations were conducted at a temperature of 300 K. The Berendsen temperature control algorithm²² with a time constant of 100 fs was used to stabilize the temperature at the borders and the bottom of the simulation cell in all simulations. Periodic boundaries were used in the two directions of the surface plane, while the bottom three layers of the substrate were fixed. Temperature was scaled smoothly over six atom layers between the fixed bottom and the remainder of the cell, in order to realistically mimic a thicker substrate.

The Cu clusters used for film growth, each containing 711 atoms and having a diameter of approximately 2.5 nm, were given the shape of Wulff polyhedra,²³ with their dimensions optimized to a configuration of minimum surface energy. Other potentials and configurations have been tested in a previous study, for which no significant differences were observed.⁷

The size of the Cu (100) substrate, $26 \times 26 \times 13$ unit cells, was chosen to be such that its length in both lateral directions would be roughly three times the diameter of the deposited clusters. The thickness of the substrate was chosen such that the substrate would be large enough to allow for energetic irradiation without too much immediate energy loss through the cell borders.

The simulation process for film growth was as follows. The clusters and substrate were created separately and allowed to relax at a constant temperature of 300 K for 50 ps before being combined. Deposition was done by giving each atom of the cluster a velocity, corresponding to a kinetic energy of 5 meV, toward the substrate. After impact of the cluster on the surface of the substrate, the film structure was allowed to relax for 100 ps before the following cluster was deposited. Between each impact, the substrate and any previously deposited cluster structure was translated randomly through the periodic boundaries of the simulation cell in order to allow for random impact points. Each cluster was rotated to a random orientation before being deposited at the center of the newly translated substrate. This process was repeated until 50 clusters had been deposited. A total of eight films were grown this way in order to collect statistics on the density of as-deposited films, as well as to allow for a large number of initial film configurations to be used in the irradiation simulations.

Irradiation was performed in a similar manner. The substrate was translated a random distance through its periodic boundaries before each ion impact, whereupon an ion of the correct species was created above the center of the substrate and given a velocity corresponding to the correct kinetic energy in a direction directly toward the substrate. Irradiation was performed in this manner to ensure that impacts would occur in random positions but sufficiently far away from the borders of the simulation cell. After each impact, the cell was relaxed for 100 ps, after which the temperature was quenched down to 300 K over the final 2 ps. The decrease in temperature during quenching was seldom more than a few tens of degrees, as most cooling had already occurred during the initial relaxation. Irradiation was continued until the densities of the films had saturated to their final levels, after approximately 100 ion impacts. Due to the size of the sub-

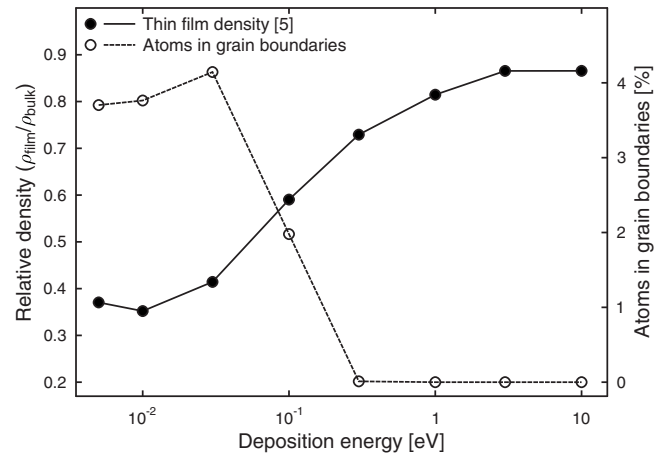


FIG. 1. Density and grain content of as-deposited cluster films, as a function of the deposition energy per atom in each cluster. Density increases toward values close to the bulk density of copper, whereas the amount of grain boundaries in the resulting films rapidly decreases to zero.

strate, each ion impact represented an approximate fluence of 1.11×10^{12} ions/cm². Irradiation was performed on all eight initial as-deposited films in order to collect statistically relevant results.

Density of the thin films was estimated by numerically calculating the amount of atoms in planar segments, starting from the bottom of the simulation cell, and comparing the mass of these atoms with the volume of the segment. The thickness of each segment was approximately one half of the lattice constant for copper. The result of these calculations was density profiles, showing the average density of each segment as a function of the vertical position of the segment from the bottom of the substrate. The zero point of these profiles was then set to coincide with the original surface of the substrate in order to ease in the distinction between substrate and deposited film. Average densities for the entire films were then calculated from the profiles as the average density for all the segments of the films. These were then compared to the average density of bulk copper, calculated to be 8.69 g/cm³, according to the specific EAM potential in use.

The nanocrystallinity of the films was estimated through the ratio of atoms in the films that were contained within grain boundaries or planar defects, such as stacking faults and twinning faults. Common neighbor analysis (CNA) was used to calculate the local crystal structure for each atom.²⁴ CNA identifies if the atoms are in local fcc or hcp crystal structure. Stacking faults are seen as two {111} planes of hcp atoms, and twin boundaries as a single such plane. In dislocation cores, the atoms are neither in hcp nor fcc crystal structure.²⁵

As a reference, grain analysis was performed on Cu₅₈₆ cluster-assembled thin films that had been produced during a previous study,⁵ regarding the effect of deposition energy on the density of thin films grown by cluster deposition. As can be seen in Fig. 1, the grain-boundary content of these cluster-assembled thin films decreased rapidly once a threshold energy of 300 meV/atom in the clusters was passed. Alternative



FIG. 2. A snapshot of a typical as-deposited film. Growth appears to be columnar, as clusters easily stick to previously deposited cluster. In some cases, depending on the orientation during impact, clusters can adopt the same crystal directions as the underlying surface, while in most cases the cluster will retain a crystal orientation separate from its surrounding. Atoms in boundaries between different crystal orientations appear slightly darker than atoms in a local fcc configuration.

methods of producing dense thin films are therefore needed if nanocrystallinity is to be preserved.

III. RESULTS

The average density of the as-deposited films was 2.67 ± 0.09 g/cm³, which is roughly 30% of the bulk density of copper according to the lattice constant given by the specific EAM potential used ($\rho_{\text{Cu}} = 8.69$ g/cm³). A film containing 50 Cu₇₁₁ clusters with this density corresponded to an average thin-film thickness of 161.4 ± 4.3 Å. The films themselves exhibited a large amount of voids between the clusters, which had retained their original crystallinity. As can be seen in Fig. 2, film growth appeared to be columnar, in accordance with experimental results,²⁶ as impacting clusters easily stuck to any clusters previously deposited.

Grain boundaries existed between most neighboring clusters, as their individual crystal orientation was unaltered at

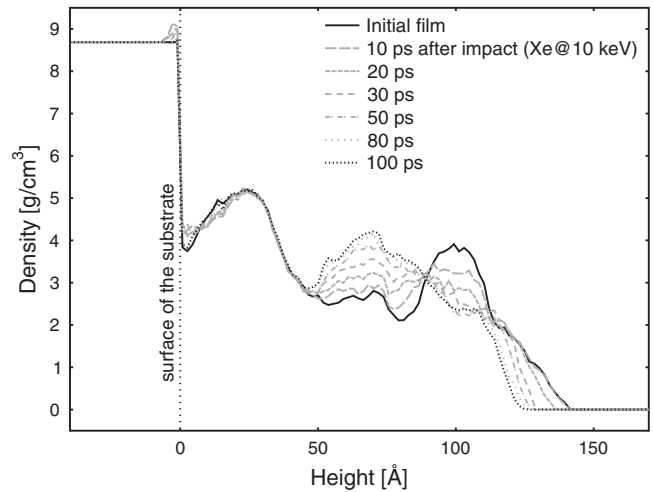


FIG. 3. A single impact of a Xe ion at 10 keV results in a huge downward transfer of mass in the initially underdense film. The solid black line shows the density profile of the as-deposited film, whereas the others indicate how the film density evolves during one Xe ion impact.

impact. Figure 2 shows a snapshot of an as-deposited film, where atoms within grain boundaries are shaded slightly darker than atoms in the fcc phase in order to enlighten this.

In Secs. III A–III E the results of heavy-ion irradiation on such porous cluster-assembled thin films will be discussed. Apart from the overall effect of irradiation on the density of the films, focus will be given to factors affecting the rate of change in density as well as to structural changes within the films. Finally, the effect of sputtering due to ion impacts will be discussed.

A. Densification

Ion irradiation resulted in a huge change within the as-deposited films, as can be seen in Fig. 3, where a single Xe ion impact, at the fairly low energy of 10 keV, has a rather remarkable effect on the structure of the porous cluster-assembled thin film. A region of higher density in the upper portions of an as-deposited film is struck by the ion, during which local melting and a transfer of a downward momentum result in a flow of viscous atoms to lower parts of the film. In effect, the entire denser region of the upper part of the film is shifted downward by almost 50 Å.

Recrystallization of the molten region is a rapid process, where most of the shift in density profile occurs during the initial 50 ps after impact. This confirms that melting and recrystallization occurs locally during irradiation, as excess kinetic energy will dissipate from the cluster-assembled film before the following ion impact.

The ion impact is also felt throughout the entire film, causing the creation of interstitial states near the surface layers of the original substrate, an effect which gives the illusion of a density higher than that of bulk copper. Diffusion of interstitials in copper at higher temperatures is however a fast process,²⁷ and the perfect structure of the substrate will return rapidly.

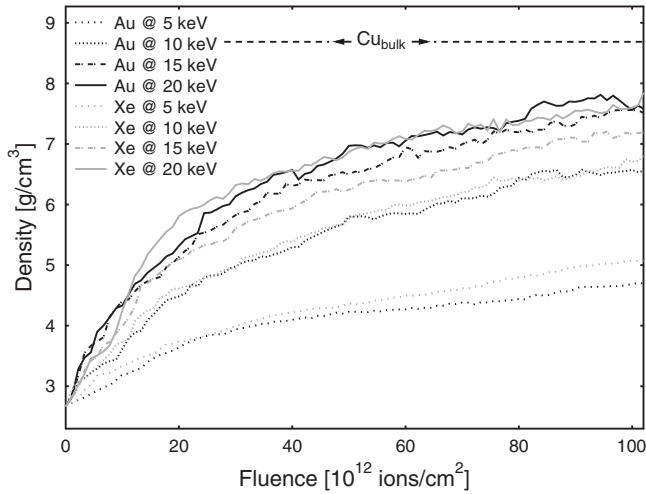


FIG. 4. The average density of irradiated films as a function of fluence. Due to the substrate size every ion impact represents an approximate fluence of 1.11×10^{12} ions/cm², hence a fluence of 100×10^{12} ions/cm² is approximately achieved with 90 ion impacts. The increase in density is initially a very rapid event, but subsides as the density of the films grows. The black lines represent irradiation with Au, while the gray lines show the effect of Xe ions. Results for the higher energies, 25–30 keV, which were approximately equal to those for 20 keV, have been left out in order to clarify the figure.

With the effect of a single ion as pronounced as can be seen in Fig. 3, it is clear that the accumulated effect of several ions will have a large impact. Figure 4 shows the average density of the irradiated films as a function of fluence, for irradiation with both Xe and Au ions at various impact energies. The average film density increases rapidly during initial irradiation for all ion energies. For the higher energies, a doubling of density is achieved at fluences as low as 15×10^{12} ions/cm². Once higher densities are achieved, however, the rate of densification subsides and density saturates to a level slightly below that of bulk copper.

Characteristic for all of the densification curves is an initial rapid, almost linear, increase in density, for fluences below 20×10^{12} ions/cm². The reasons for this are discussed in detail in Secs. III B–III E. Crucial differences for irradiation with the different species, Xe and Au, cannot be noticed within the margins of error, which are approximately 0.25 g/cm^3 for all values of density. For the low irradiation energies, 5 and 10 keV, densities remain fairly low throughout irradiation, whereas significant changes in the densification rates cannot be seen once irradiation energies surpass 15 keV. The final densities for all films irradiated with energies above 15 keV are equal, within the margins of error, irrespective of the ion species.

B. Ion ranges and energy deposition

The differences in rate of densification between Xe and Au are only slight and even seem to coincide within the margins of error. From Fig. 4, it can be seen that the rate of densification is slightly higher for Xe at the lower energies, but slightly lower once the energy increases above 15 keV.

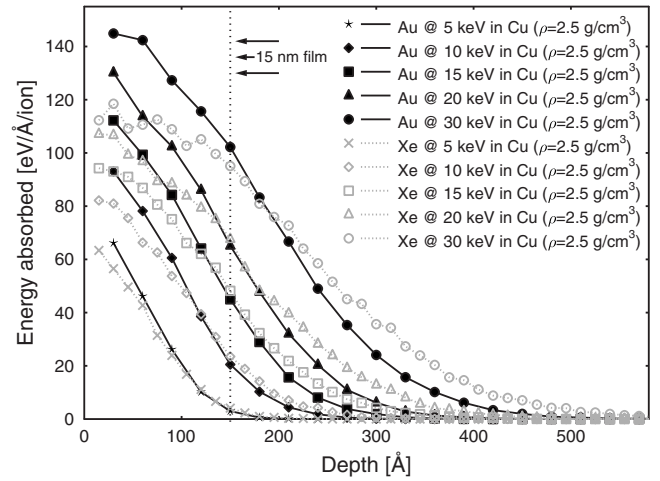


FIG. 5. Energy deposition as a function of depth, calculated using SRIM, for various ions impacting on underdense copper. The dotted vertical line shows a thickness of 15 nm, which was the approximate thickness of thin films used in these simulations. The fairly low deposition of energy at a higher depth, seen for ions with kinetic energy below 15 keV, did not result in a satisfactory densification of the entire films.

This can be explained by considering the range and energy deposition of the respective ions in copper.

Figure 5 shows the energy deposition for Xe and Au at different energies in under-dense copper ($\rho = 2.5 \text{ g/cm}^3$), calculated with binary collision approximation using the computer program SRIM.^{28,29} The range of Xe in copper is higher than that of Au, which results in a slightly larger deposition of energy at the lower layers of a film with a thickness of 150 Å. At higher energies, the ranges of both Xe and Au ions are such that energy is deposited throughout the entire films. At these energies, 15 keV and above, the amount of deposited energy per ion is higher for Au, resulting in a faster densification process.

The difference in the densification process between low- and high-energy ions can easily be seen from Figs. 6 and 7, showing snapshots and density profiles from two films after irradiation by different amounts of ions. Figure 6 shows the state of thin films before irradiation and after having been irradiated with 10, 20, 40, and 60 Xe ions at an energy of 25 keV/ion. The upper portions of the film are rapidly compressed, forming a denser layer approximately 70 Å above the surface.

When irradiation is continued, the lower portions of the film are also pressed downward as the flow of atoms is able to cause a filling of voids. Once the amount of impacts has approached 40 Xe ions, the density of the thin film is almost equal to that of bulk copper. The effect of further irradiation can only be seen as a smoothening of the film surface.

In Fig. 7, the state of thin films before and after irradiation by 10, 20, 40, and 60 Xe ions at an energy of 5 keV/ion can be seen. The energy deposition per ion is naturally much lower for Xe at 5 keV than the same ion at five times the energy. This can be seen in the slower change in the upper portions of the film. Only after approximately 20 impacts have the clusters in the higher portions of the film sintered

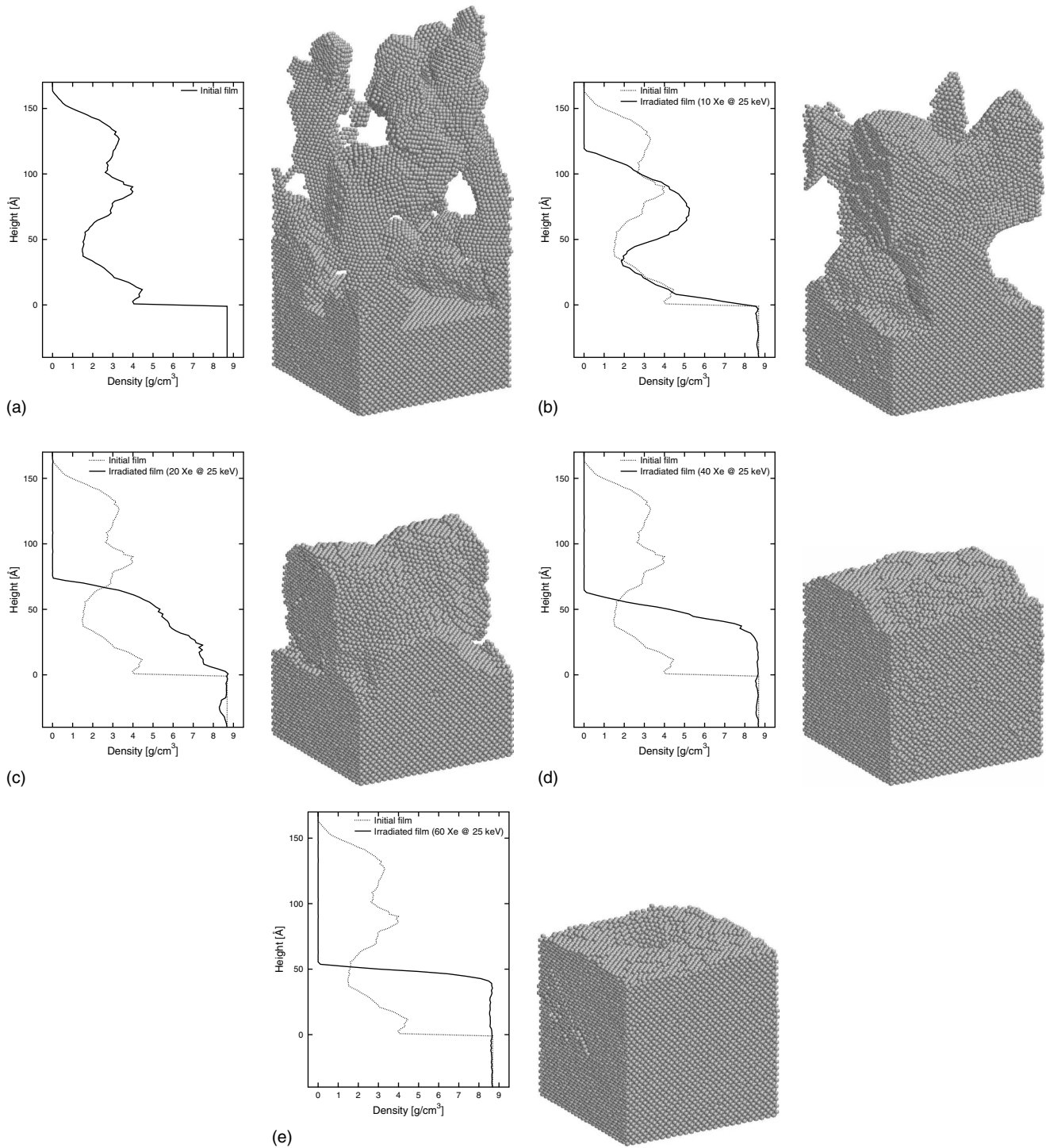


FIG. 6. Snapshots of a thin film during bombardment with Xe at 25 keV, together with density profiles for each case. (a) The initial film and the same film after (b) 10, (c) 20, (d) 40, and (e) 60 ion impacts.

into a compressed structure. This structure slowly continues to flow downward, although the lower portions of the film continue to remain at a lower density than its surrounding. This is due to the shallow range of Xe ions at this low energy, hindering the deposition of energy to these lower layers.

If densification of the complete film is required, ion energies should be chosen such that their range at the least is of the same order as the thickness of the film. A higher deposi-

tion of energy will result in a faster densification, which therefore favors the use of heavy projectiles.

C. Surface roughness

As can be seen from Fig. 8, where the density profile of a thin film is plotted during irradiation with Xe at 15 keV, the film density in the lower layers of the film equals that of bulk copper even after a fairly low amount of ion impacts. A

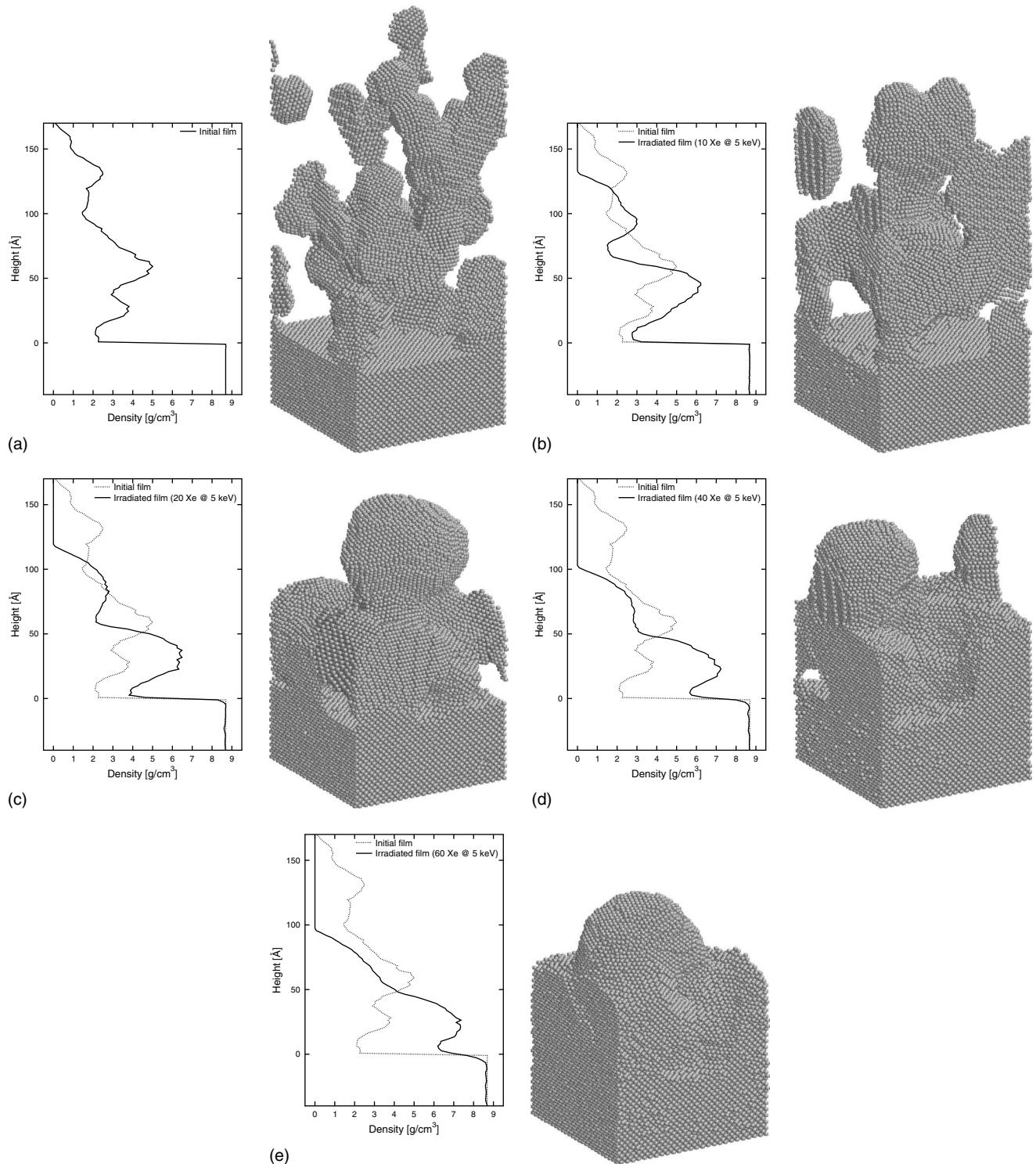


FIG. 7. Snapshots of a thin film during bombardment with Xe at 5 keV, together with density profiles for each case. (a) The initial film and the same film after (b) 10, (c) 20, (d) 40, and (e) 60 ion impacts.

substantial reason for low calculated average film densities is a shallow slope in the topmost layers of the density profile. This slope corresponds to surface roughness, which remains even after irradiation.

The true density of the thin film is in fact not affected by the surface roughness, which should therefore not be accounted for in the calculations on average film density. Fig-

ure 9 shows the average density of the thin films as a function of fluence, when irradiated by both Au and Xe ion species, for the case where the topmost 15% of the thickness of the thin film is considered to be a surface layer, and therefore left out of the calculations. From Fig. 8, it is evident that 15% is a rather conservative estimate for the thickness of the surface layer, as the density profile after 50 ion impacts ex-

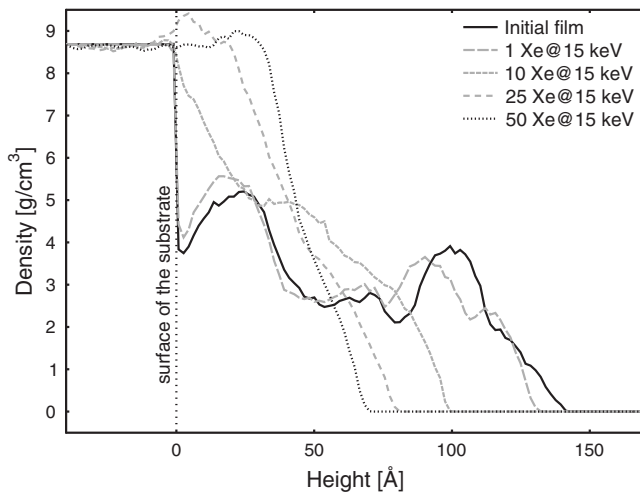


FIG. 8. Density profile of a thin film after irradiation with increasing amounts of Xe ions at an energy of 15 keV. Initial film density is 2.98 g/cm^3 , whereas the average density after 50 ion impacts has grown to 5.96 g/cm^3 . The seemingly low value for the density of the irradiated film is almost entirely due to surface roughness.

hibits a smooth decreasing slope between a height of $35\text{--}70 \text{ \AA}$, which is approximately half of the height of the thin film. A surface layer of only 15% of the film thickness was however chosen in order to allow for a larger part of the atoms of the film to be included in the density calculations.

A surface layer with a thickness of half the total film height, if its density smoothly decreases as a function of height, contains approximately 30% of the atoms of the film. In the case of a surface layer with a thickness only 15% of that of the film, if its density similarly decreases smoothly with height, as little as 8% of the atoms of the film would be discarded from the density calculations.

From Fig. 9, it can easily be seen that the true density of the irradiated films in fact approaches the bulk density of copper at fairly low fluences. For the higher irradiation energies, bulk density would be achieved even earlier if a thicker surface layer was discarded from the average density calculations. This is most evident for irradiation with Xe ions, as compared to Au ions, because a more even distribution of energy deposition throughout the underdense films allows for a rapid densification before smoothing of the surface is initiated.

For Xe ions at energies above 20 keV, a sharp kink in the densification curves can be seen at a fluence of approximately $20 \times 10^{12} \text{ ions/cm}^2$. Initially, there is a rapid increase in density at fluences below $20 \times 10^{12} \text{ ions/cm}^2$, which corresponds to a densification of the whole film. After this the rate of densification decreases at higher fluences, as voids within the film have been filled and only surface smoothing takes place. The surface layer is however initially rather thick, and only at a fluence of $80 \times 10^{12} \text{ ions/cm}^2$ does the under-dense surface layer shrink to below 15% of the film thickness.

D. Grains

The amount of atoms within grain boundaries inside the films was calculated with CNA throughout the irradiation

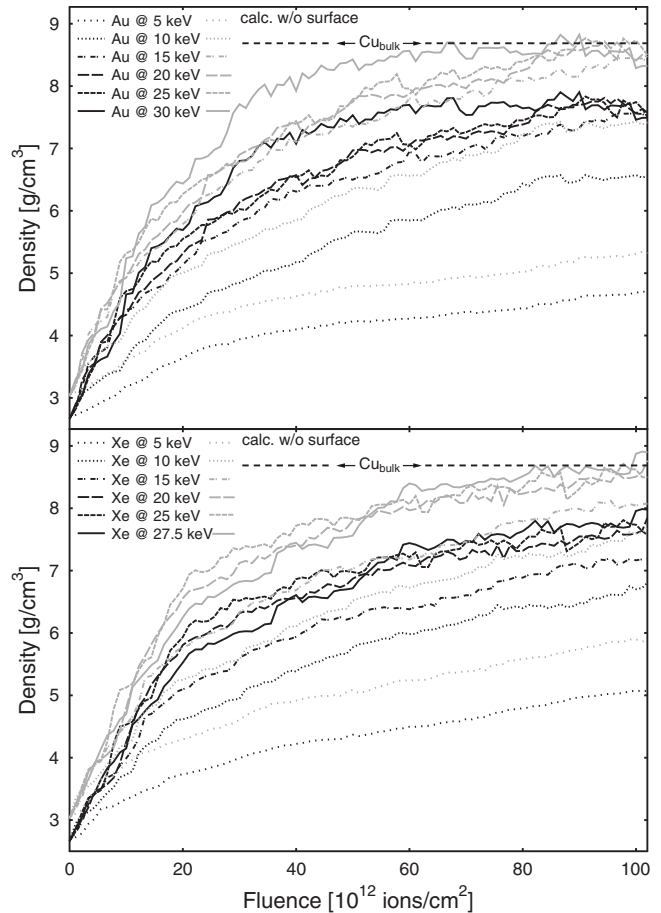


FIG. 9. The average density of the entire thin films, visualized using black lines, is compared to their calculated densities when the topmost 15% of the thin film is removed, shown as gray lines, in order to lessen the effect of surface roughness.

process in order to monitor if nanocrystallinity of the thin films was heavily affected by the heavy-ion irradiation.

As the decisive mechanism causing densification is the melting and recrystallization of local regions within the thin films, it is only natural to presume that grain growth will also occur. Grain growth has likewise been reported in several theoretical and experimental papers focused on changes in morphology during the irradiation of nanocrystalline samples.^{30–33}

Figure 10 shows the results of the CNA analysis, plotted as the percentage of film atoms contained within grain boundaries as a function of the irradiation fluence. For all energies and ion species, the amount of atoms in grain boundaries does indeed decrease as fluence is increased. However, if compared to the relationship between density and grain amount in as-deposited films (as was indicated in Fig. 1), grains remain present in the films throughout irradiation, and even at a fairly large amount.

As the thin films are compressed during the densification process, single clusters will sinter with others, and therein adopt a different orientation. Because melting occurs locally, and recrystallization is such a fast process, several crystal orientations will however remain within the film, as grains with different orientations will simultaneously grow in sev-

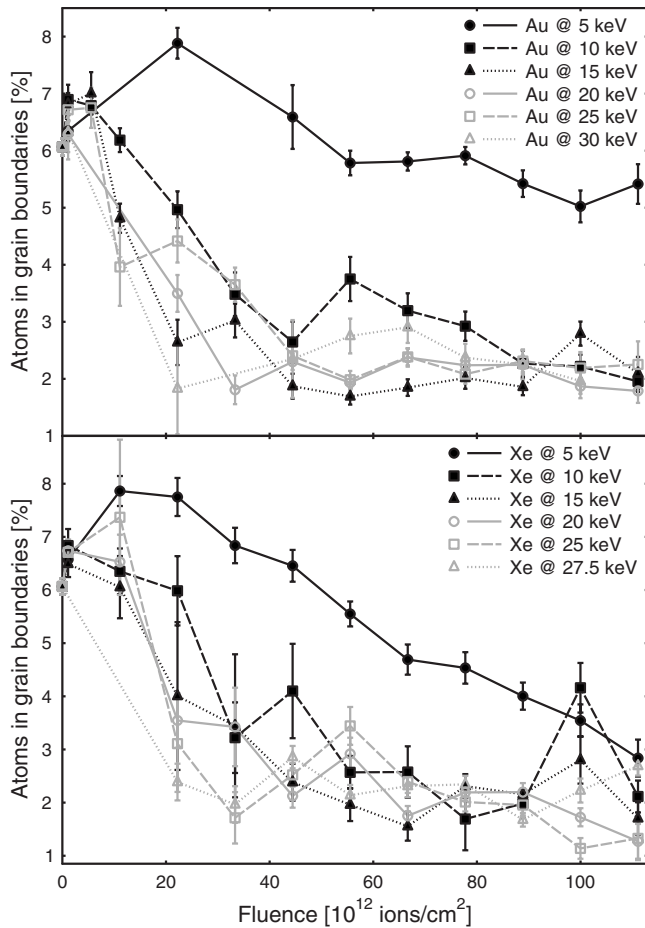


FIG. 10. The amount of atoms within grain boundaries for thin films irradiated at different energies with Au and Xe ions, as a function of fluence. Even though the amount of atoms in grain boundaries decreases during irradiation, no irradiation energy results in a complete deletion of grain boundaries. All samples remained nanocrystalline although grain growth was promoted.

eral locations. If a global melting had occurred, recrystallization would proceed according to some predominant orientation, thereby resulting in the growth of very much larger grains.

For the case of irradiation at 5 keV, the initial effect is an increase in the amount of atoms within grain boundaries, and only after this does the amount of atoms within grain boundaries slowly decrease. This appears contradictory, as all other irradiation energies resulted in the rapid decrease in the amount of atoms in grain boundaries during initial irradiation. After the initial rapid decrease, the grain-boundary content appears to remain fairly constant throughout further irradiation with the higher energy ions. The reason for this discrepancy between 5 keV irradiation and irradiation at higher energies is the much smaller region of local melting within the films caused by low-energy ion impacts.

Because only small parts of clusters melted during irradiation with 5 keV ions, a viscous downward flow and recrystallization of these atoms did not really affect the amount of grains within the films, but rather only their individual positions. In the initial stages of irradiation, when individual clusters only have small contact areas with their neighbors,

the amount of atoms in boundaries between these clusters will naturally be smaller than it will be once the clusters are closer to each other in a slightly densified film. This effect will cause the increase in grain content seen for irradiation of the films at 5 keV, with both Au and Xe ions. Once clusters in the densified films had slightly larger contact areas with their neighbors than originally, local melting was more likely to occur at grain boundaries, therein improving the opportunity for complete annihilation of some of the individual grains. For this reason, however, films densified with low-energy irradiation retained a larger part of their grain boundaries than their high-energy irradiated counterparts.

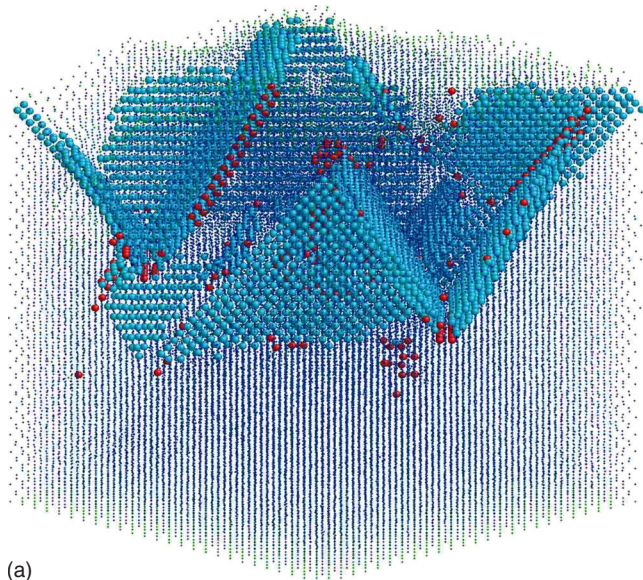
This difference is illustrated in Fig. 11, which shows snapshots of two densified thin films, irradiated with Au ions at 30 and 5 keV, respectively. Grain boundaries between regions with different crystal directions are visualized as somewhat larger atoms. From the snapshots, differences in structure between films irradiated with high-energy and low-energy ions can clearly be seen. In the case of high-energy irradiation, several parts of the thin film have recrystallized at orientations different from the underlying substrate, although grain sizes are clearly much larger than the size of the original clusters. After low-energy irradiation, grain sizes have grown beyond the original size of the cluster, but remain much smaller than for high-energy irradiation.

The existence of several different crystal orientations, as seen in the snapshots, confirms the fact that the cluster-assembled films retain nanocrystallinity throughout the densification process. Although the grain size has undoubtedly grown, these are still rather small. It is, however, clear that their final size will be very much dependent on the original size of the deposited clusters and the energy at which the films are irradiated.

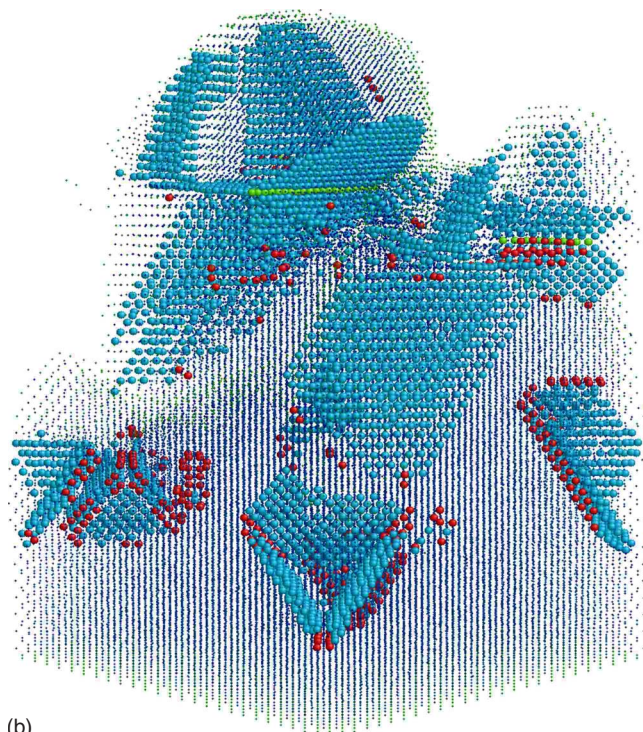
E. Sputtering

At ion energies and fluences as low as the ones used for irradiation in these simulations, sputtering of copper is not of crucial importance. For reassurance in this matter, sputtering yields during irradiation were nonetheless monitored. The results can be seen in Fig. 12, where the sputtering yield as a function of ion energy is plotted for both ion species. Different data sets are used for the cases where average film densities are below and above a threshold density of 6.0 g/cm^3 . At densities below this value, larger aggregates could sometimes be sputtered from the films, as large parts of still ascertainable individual clusters were detached from the films. At higher densities, the likelihood for such events was minimal. This effect also seemed to be energy dependent, as sputtering yields for the underdense films increased as ion energy increased, but only up to a specific point. Once ion energies, and therefore ion ranges, were too high, sputtering yields decreased. This can be explained by the fact that atoms sputtered from lower parts of underdense films were captured by the upper parts of those films.

Sputtering yields were also higher for the heavier ion Au as compared to those of Xe. For both ion species, the yields were however low enough to allow for less than 3% of the films to be sputtered away during irradiation. Sputtering



(a)



(b)

FIG. 11. (Color online) A snapshot showing dislocations and grain boundaries present in a film after (a) irradiation with Au ions at an energy of 30 keV and a fluence of approximately 60×10^{12} ions/cm², and (b) after irradiation with Au ions at an energy of 5 keV and a fluence of 100×10^{12} ions/cm². Atoms within stacking faults and twin boundaries are shown as slightly larger than atoms within a fcc configuration.

yields from thin films with density above 6.0 g/cm³ were well within the range of experimental values.³⁴

IV. DISCUSSION

A rapid increase in density of the as-deposited cluster films was achieved with a fairly low irradiation fluence.

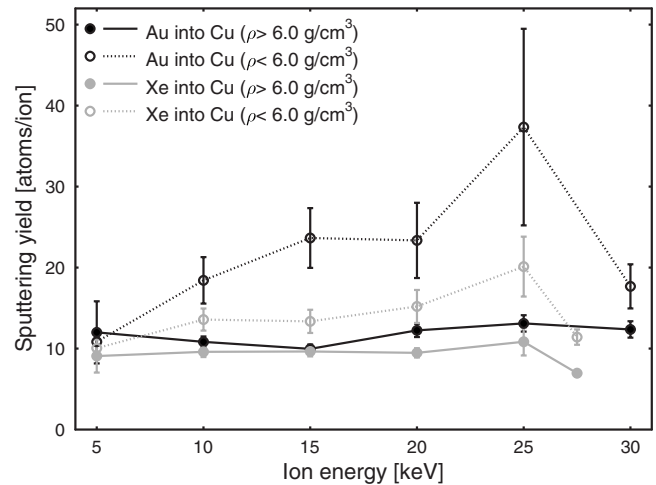


FIG. 12. The sputtering yield as a function of ion energy for Xe and Au projectiles impacting on Cu films with densities either below or above 6.0 g/cm³. Overall sputtering yields are fairly low, which would indicate that the loss of film material is not too great throughout the densification process. The sputtering yield is somewhat higher for underdense films (dotted lines), as the likelihood for larger parts of film to be sputtered in clusters is greater.

Even though irradiation was continued for a considerably higher fluence, nanocrystallinity was preserved within the films. This allowed for the creation of dense films with a greater degree of nanostructure than those grown by variation in cluster deposition energies.

Thin-film growth and densification were performed for only one cluster size in this work. Variations in the size of the deposited clusters would naturally affect the results to some extent. The density of as-deposited films is at least in some way dependent on cluster size, as the behavior of single clusters deposited on a smooth surface varies greatly with the size of the clusters.⁷ Smaller clusters may very likely form a denser as-deposited film, as they tend to rearrange upon impact due to the release of binding energy, which originates from a decrease in the surface energy.^{8,9} If larger clusters are used, densities of the as-deposited films may remain somewhat similar, although their use would affect the results in another way.

For larger clusters, irradiation with ions at a higher energy is required in order to cause similar viscous flow of material toward lower parts of the film. Smaller molten regions caused by impacts at lower irradiation energies would only recrystallize within the original clusters, and densification would only be a minor effect. In order to achieve molten regions large enough to cause the flow of a considerable part of an individual cluster, energy deposition per ion would have to be much higher. Further study is needed in order to examine the optimal ion energy if cluster sizes and film thicknesses are varied.

Long-time-scale thermally activated events may also affect the results of this study, as properties of the as-deposited cluster films may vary if clusters have more time to evolve on the surface.^{10,35} Deposition of clusters on a substrate area of about 90 nm² at a rate of one every 100 ps corresponds to a flux of roughly 10^{22} clusters/(cm² s), which is about 3

orders of magnitude higher than the highest fluxes achieved with any contemporary method (plasma machines can achieve fluxes of the order of 10^{19} ions/(cm² s) (Ref. 36) and several orders of magnitude higher than that of any existing cluster deposition equipment.

The rates of thermally activated events are, however, inversely related to the size of the clusters. Small clusters will therefore be flattened out much more rapidly than larger ones. From previous work in our group, we know the time scale by which Cu nanoclusters flatten out on Cu surfaces,³⁷ which allows us to estimate that, given typical cluster deposition fluxes of the order of 10^{12} – 10^{15} clusters/(cm² s), the present results are valid for deposition with smaller clusters (containing less than 200 atoms) up to temperatures of about 300–500 K, and for larger clusters at much higher temperatures.

A calculation similar to that of the cluster deposition flux might also be used for calculating the flux during heavy-ion irradiation, as substrate size and ion impact frequency is the same. The calculation is, however, complicated by that fact that the temperature of the thin films was quenched down to 300 K between each ion impact. This makes it difficult to properly estimate a corresponding experimental flux, although it is evident that it would be much lower than that of cluster deposition.

As the simulations were performed under ideal circumstances, some neglected aspects of experimental procedures may also affect the outcome. If deposition and irradiation is performed with rapid succession in ultrahigh-vacuum (UHV) conditions, oxidation will not be a severe problem. If a poorer vacuum is used, or if samples are transported through atmospheric conditions between deposition and irradiation, a layer of metal oxide will, however, undoubtedly form around each individual cluster. This could have consequences for the recrystallization of molten regions during irradiation, and intermixing of oxide and pure metal will very likely occur. Densification rates will probably be affected by the presence of oxides, as will nanocrystallinity, although the latter might indeed increase if borders between individual clusters are more differentiated. The mechanical properties of the final films will also most probably be affected by the presence of metal oxides.

Despite the few doubts that still remain, this work brings forth a method for the production of nanostructured thin films. Densification of cluster-assembled thin films is a gentle method of film growth that can be used for almost any substrate, as low-energy cluster deposition is a gentle process

that can be carried out at room temperature, and irradiation, at energies and fluences as low as the ones used in this work, hardly does any damage at all. This method offers better mechanical properties and adhesion than what can be achieved through film growth by low-energy deposition of nanoclusters, but still allows for the utilization of the nanoscale size of the clusters themselves. The combination of low-energy cluster deposition and heavy-ion irradiation of the as-deposited films is a promising method for the growth of nanocrystalline thin films on almost any surface.

Due to the nature of nanocluster formation in many cluster sources, through condensation of vaporized material, this method also opens up another opportunity for the growth of exotic nanocrystalline thin films.³⁸ An interesting effect of the far-from-equilibrium condensation which occurs in cluster sources is the growth of bimetallic cluster of almost any stoichiometric composition.^{39,40} Segregation of the elements in any alloyed thin films is of great concern if deposition or modification is carried out at higher temperatures. At low temperatures, such as room temperature and below, diffusion is limited and elements may remain in a mixed phase. Deposition of bimetallic clusters at low energies and the subsequent irradiation of these structures may allow for the growth of dense alloyed thin films, and if segregation during irradiation is not too severe, perhaps even alloyed films of immiscible metals.

V. CONCLUSIONS

Using molecular-dynamics simulations we have grown porous thin films by low-energy cluster deposition and subsequently densified them through heavy-ion irradiation. Irradiation of cluster-assembled thin films was proved a feasible method of densification if nanocrystallinity and gentleness toward the substrate are of importance.

Densities approaching those of bulk copper, in originally underdense thin films, were achieved by irradiation with Xe and Au ions at energies between 5 and 30 keV and fluences in the order of 10^{13} ions/cm². Nanocrystallinity was preserved in the thin films throughout irradiation.

ACKNOWLEDGMENTS

This work was performed within the Finnish Centre of Excellence in Computational Molecular Science (CMS), financed by The Academy of Finland and the University of Helsinki. We also gratefully acknowledge the grants of computer time from CSC, the Finnish IT center for science.

*kristoffer.meinander@helsinki.fi

¹H. Haberland, M. Karrais, M. Mall, and Y. Thurner, *J. Vac. Sci. Technol. A* **10**, 3266 (1992).

²H. Haberland, M. Mall, M. Moseler, Y. Qiang, T. Reinert, and Y. Thurner, *J. Vac. Sci. Technol. A* **12**, 2925 (1994).

³H. Haberland, Z. Insepov, M. Karrais, M. Mall, M. Moseler, and Y. Thurner, *Nucl. Instrum. Methods Phys. Res. B* **80-81**, 1320

(1993).

⁴K. Meinander, K. Nordlund, and J. Keinonen, *Nucl. Instrum. Methods Phys. Res. B* **242**, 161 (2006).

⁵K. Meinander, T. Clauß, and K. Nordlund, in *Growth, Modification, and Analysis by Ion Beams at the Nanoscale*, MRS Symposium Proceedings No. 908E, edited by W. Jiang (MRS, Warrendale, PA, 2006), p. 0908-OO14-20.1.

- ⁶K. Nordlund, T. T. Järvi, K. Meinander, and J. Samela, *Appl. Phys. A: Mater. Sci. Process.* **91**, 561 (2008) invited paper.
- ⁷K. Meinander, J. Frantz, K. Nordlund, and J. Keinonen, *Thin Solid Films* **425**, 297 (2003).
- ⁸K. Meinander, T. T. Järvi, and K. Nordlund, *Appl. Phys. Lett.* **89**, 253109 (2006c).
- ⁹T. T. Järvi, A. Kuronen, K. Meinander, K. Nordlund, and K. Albe, *Phys. Rev. B* **75**, 115422 (2007).
- ¹⁰P. Moskovkin and M. Hou, *Eur. Phys. J. D* **27**, 231 (2003).
- ¹¹P. G. Sanders, G. E. Fougere, L. J. Thompson, J. A. Eastman, and J. R. Weertman, *Nanostruct. Mater.* **8**, 243 (1997).
- ¹²M. Nastasi, J. Mayer, and J. Hirvonen, *Ion-Solid Interactions—Fundamentals and Applications* (Cambridge University Press, Cambridge, Great Britain, 1996).
- ¹³C. A. Volkert, *J. Appl. Phys.* **70**, 3521 (1991).
- ¹⁴C. M. Lopatin, T. L. Alford, V. B. Pizziconi, M. Kuan, and T. Laursen, *Nucl. Instrum. Methods Phys. Res. B* **145**, 522 (1998).
- ¹⁵M. Ghaly and R. S. Averback, *Phys. Rev. Lett.* **72**, 364 (1994).
- ¹⁶M. Samaras, P. M. Derlet, H. V. Swygenhoven, and M. Victoria, *J. Nucl. Mater.* **323**, 213 (2003).
- ¹⁷M. Samaras, P. M. Derlet, H. V. Swygenhoven, and M. Victoria, *J. Nucl. Mater.* **351**, 47 (2006).
- ¹⁸M. P. Allen and D. J. Tildesley, *Computer Simulation of Liquids* (Oxford University, Oxford, England, 1989).
- ¹⁹M. S. Daw and M. I. Baskes, *Phys. Rev. B* **29**, 6443 (1984).
- ²⁰S. M. Foiles, M. I. Baskes, and M. S. Daw, *Phys. Rev. B* **33**, 7983 (1986).
- ²¹J. F. Ziegler, J. P. Biersack, and U. Littmark, *The Stopping and Range of Ions in Matter* (Pergamon, New York, 1985).
- ²²H. J. C. Berendsen, J. P. M. Postma, W. F. van Gunsteren, A. DiNola, and J. R. Haak, *J. Chem. Phys.* **81**, 3684 (1984).
- ²³J. E. Hearn and R. L. Johnston, *J. Chem. Phys.* **107**, 4674 (1997).
- ²⁴J. D. Honeycutt and H. C. Andersen, *J. Phys. Chem.* **91**, 4950 (1987).
- ²⁵J. Schiøtz, *Scr. Mater.* **51**, 837 (2004).
- ²⁶H. Haberland, Z. Insepov, and M. Moseler, *Phys. Rev. B* **51**, 11061 (1995).
- ²⁷J. Steigman, W. Shockley, and F. C. Nix, *Phys. Rev.* **56**, 13 (1939).
- ²⁸J. P. Biersack and L. G. Haggmark, *Nucl. Instrum. Methods* **174**, 257 (1980).
- ²⁹J. F. Ziegler, SRIM-2003 software package, <http://www.srim.org>
- ³⁰S. G. Mayr and R. S. Averback, *Phys. Rev. B* **68**, 075419 (2003).
- ³¹W. Voegeli, K. Albe, and H. Hahn, *Nucl. Instrum. Methods Phys. Res. B* **202**, 230 (2003).
- ³²D. Kaoumi, A. T. Motta, and R. C. Birtcher, *Nucl. Instrum. Methods Phys. Res. B* **242**, 490 (2006).
- ³³N. Nita, R. Schaeublin, M. Victoria, and R. Z. Valiev, *Philos. Mag.* **85**, 723 (2005).
- ³⁴A. Oliva-Florio, R. A. Baragiola, M. M. Jakas, E. V. Alonso, and J. Ferrón, *Phys. Rev. B* **35**, 2198 (1987).
- ³⁵P. Jensen and N. Combe, *Comput. Mater. Sci.* **24**, 78 (2002).
- ³⁶A. Brunelle and S. Della-Negra, *Nucl. Instrum. Methods Phys. Res. B* **222**, 68 (2004).
- ³⁷J. Frantz, M. Rusanen, K. Nordlund, and I. T. Koponen, *J. Phys.: Condens. Matter* **16**, 2995 (2004).
- ³⁸K. S. Kumar, H. V. Swygenhoven, and S. Suresh, *Acta Mater.* **51**, 5743 (2003).
- ³⁹R. L. Wagner, W. D. Vann, and J. A. W. Castleman, *Rev. Sci. Instrum.* **68**, 3010 (1997).
- ⁴⁰P. Milani and S. Iannotta, *Cluster Beam Synthesis of Nanostructured Materials*, Springer Series in Cluster Physics (Springer-Verlag, Berlin, 1999).